BASIC SCIENCE

Nanomedicine: Nanotechnology, Biology, and Medicine
14 (2018) 1 – 12

Original Article

nanomedjournal.com

Gold nanoparticles: Distribution, bioaccumulation and toxicity. *In vitro* and *in vivo* studies

Carlos Lopez-Chaves, PhD[a,1], Juan Soto-Alvaredo, PhD[b,1], Maria Montes-Bayon, PhD[b], Jörg Bettmer, PhD[b,*], Juan Llopis, PhD[a], Cristina Sanchez-Gonzalez, PhD[a,**]

[a]*Biomedical Research Centre, iMUDS, Institute of Nutrition and Food Technology "José Mataix", Department of Physiology, Faculty of Pharmacy, University of Granada, Campus Cartuja, Granada, Spain*

[b]*Department of Physical and Analytical Chemistry, University of Oviedo, C/ Julian Clavería 8, Oviedo, Spain*

Received 2 December 2016; accepted 16 August 2017

Abstract

Concerns about the bioaccumulation and toxicity of gold nanoparticles inside humans have recently risen. HT-29 and HepG2 cell lines and Wistar rats were exposed to 10, 30 or 60 nm gold nanoparticles to determine their tissue distribution, subcellular location and deleterious effects. Cell viability, ROS production and DNA damage were evaluated *in vitro*. Lipid peroxidation and protein carbonylation were determined in liver. ICP-MS measurements showed the presence of gold in intestine, kidney, liver, spleen, feces and urine. Subcellular locations of gold nanoparticles were observed in colon cells and liver samples by transmission electron microscopy. Inflammatory markers in liver and biochemical parameters in plasma were measured to assess the inflammatory status and presence of tissue damage. The size of the nanoparticles determined differences in the biodistribution and the excretion route. The smallest nanoparticles showed more deleterious effects, confirmed by their location inside the cell nucleus and the higher DNA damage.

Key words: Gold nanoparticles; Oxidative stress; Inductively couple plasma-mass-spectrometry; Toxicity

Nanomaterials, defined as any material possessing at least one dimension in the nanometer scale between 1 and 100 nm, are found to have many uses and potential applications in the fields of biology and medicine. The specific physico-chemical properties at the nanoscale are expected to result in an increased reactivity with biological systems. So, in addition to their beneficial effects, engineered nanoparticles of different types may also represent a potential hazard to human health. The need to understand nanoparticles in a biological environment is now shared by nanobiology, nanomedicine and nanotoxicology. Thus, nanotoxicity is an emerging field of research, a response to growing uses of nanosized materials in a slew of technological applications and consumer products.

Gold in its native form has long been considered an inert, noble metal with some therapeutic and even medicinal value; hence gold nanoparticles (AuNPs) are also thought to be relatively non-cytotoxic. Thereby, the exposure to AuNPs by humans has enormously increased during last decades due to their use in multiple areas like electronics and sensors,[1] solar cells[2] or catalysis,[3] but especially in biomedical applications like radiotherapy,[4,5] as drug carriers or in cancer therapies.[6,7] However, despite the huge potential benefit of AuNPs in the areas of biomedical and industrial applications, there has been an increased interest in studying their possible deleterious effects in biological systems and how these effects might be mitigated. Different characteristics such as diameter, coating,[5] shape,[8]

This work was supported by the Spanish Ministry for Science and Innovation (Grant Number CTQ2011-23038) and the Spanish Ministry for Education, Culture and Sports (Grant Number FPU13/00062). These results are included in the PhD thesis of Carlos López Chaves from the University of Granada, Nutrition and Food Sciences doctoral program.

The authors have no conflicts of interest to declare.

*Correspondence to: J. Bettmer, Department of Physical and Analytical Chemistry, C/ Julian Clavería 8, University of Oviedo, E-33006 Oviedo, Spain.

**Correspondence to: C. Sanchez-Gonzalez, Department of Physiology, Campus Cartuja, University of Granada, Granada, Spain.

E-mail addresses: bettmerjorg@uniovi.es (J. Bettmer), crissg@ugr.es (C. Sanchez-Gonzalez).

[1] These authors contributed equally in this work.

http://dx.doi.org/10.1016/j.nano.2017.08.011
1549-9634/

Please cite this article as: Lopez-Chaves C, et al, Gold nanoparticles: Distribution, bioaccumulation and toxicity. *In vitro* and *in vivo* studies. *Nanomedicine: NBM* 2018;14:1-12, http://dx.doi.org/10.1016/j.nano.2017.08.011

dose[9] or route of administration[10] have demonstrated to be essential in the distribution,[11,12] accumulation,[13] metabolism,[5] elimination[5,14] and therefore effects and toxicity of these nanoparticles.

Previous studies have been conducted to evaluate the toxicity of different nanostructured gold compounds. Particularly, the metallic nature of the AuNPs and the presence of the transition metals core encourage the production of reactive oxygen species (ROS) leading to oxidative stress.[8,15] Furthermore, once these nanoparticles enter a biological system, they can strongly associate with a diverse range of molecules present in the extra- and intracellular environment. Among them, lipids, nucleotides, low-molecular-weight species, and especially proteins are known to establish strong interactions with these nanoparticles, which could cause an imbalance in the oxidative status and therefore the function of these molecules. Thus, Thakor et al observed that after treating HepG2 cells with AuNPs, at the relatively early time points, there were increases in antioxidant enzyme concentrations, which appeared to balance any deleterious effects associated with ROS, thereby protecting the cell.[8] Although the antioxidant enzyme concentrations continued to increase over time, the amount of ROS produced most likely overwhelmed these antioxidant defenses since HepG2 cells demonstrated evidence of oxidative stress-induced damage with increased tissue phospholipid and protein oxidation. Moreover, Li et al showed that AuNPs inhibit cell proliferation by downregulating cell cycle genes.[16] Furthermore, AuNPs not only seems to cause oxidative damage but also affect genes associated with genomic stability and DNA repair. The hypothesis could be that while AuNPs treatment induces oxidative stress, the cells may be able to avoid cell death through autophagic pathways. It is also likely that the oxidative environment could trigger off the autophagic process, rather than a direct cellular reaction to AuNPs presence in the cell.[15] Nevertheless, other researchers have observed no sign of oxidative stress after administering AuNPs to cell cultures[17] or even a decrease in oxidative stress markers.[18] In this sense, the effect of gold nanoparticles on the oxidative status remains unclear.

The distribution of the incorporated nanoparticles inside the body over the various organ systems and within the organs needs to be determined. De Jong et al demonstrated that the fate of AuNPs after intravenous administration depends on their size.[12] According to their results, the smallest particle studied, 10 nm, revealed the most widespread tissue distribution at 24 h after injection, while bigger AuNPs were found to be present in liver, spleen and blood. In any case, liver seemed to have the highest concentration of AuNPs. On the other hand, *in vitro* studies performed to determine the intracellular distribution of these nanoparticles, show that AuNPs seem to aggregate in endosomal/lysosomal vesicles but not in organelles, such as the nucleus; and that endocytosis seem to be the main route of entry.[9,16,17,19,20]

The evaluation of the effect of these nanoparticles on the regulation of the inflammatory and biochemical processes has been controversial. Some authors note that the exposure to AuNPs up-regulates the expression of pro-inflammatory cytokines like IL-1, IL-6 or TNF-α the overexpression is size-dependent[20,21]; while other studies propose that the inflammatory response is rapidly normalized after an initial acute phase, reaching normal levels after a short-period treatment.[13,22] Furthermore, several biochemical parameters have been measured in order to determine the damage of AuNPs.[23,24]

The aim of this study was to clarify (both *in vitro* and *in vivo*) the tissue distribution, subcellular location and deleterious effects of three different sizes of AuNPs by means of the analysis of the content of Au in tissues, image studies and the determination of oxidative stress, inflammatory and tissue damage markers.

Methods

Gold nanoparticles

Citrate-stabilized gold nanoparticles with 10, 30 or 60 nm of diameter size, suspended in ultrapure water at 50 mg/L, were purchased at the National Institute of Standard and Technology (NIST RM 8011, 8012 and 8013, Gaithersburg, USA). The reference values obtained by TEM were 8.9 ± 0.1, 27.6 ± 2.1, and 56.0 ± 0.5 nm respectively. In order to confirm the presence of monodisperse Au nanoparticles, the purchased materials were regularly checked in our laboratory. The lowest dose of AuNPs used in the present study is one of the most employed in toxicity assays in literature.[17,24] The highest dose was chosen in order to evaluate the possible negative effects.

In vitro studies

Cell culture conditions

HepG2 and HT-29 cell lines were obtained from the Cell Culture Resource Centre at the University of Granada, Spain. The cells were precultured in 25cm^2 culture flasks in RPMI-1640 medium (containing 2.0 mg mL^{-1} sodium bicarbonate) supplemented with 10% (v/v) FBS and 2 mM L-glutamine. The culture flasks were maintained in a cell incubator at 37 °C in a humidified atmosphere of 5% CO_2 and 95% air. Medium was replaced every 2-3 days after rinsing with PBS. Upon reaching confluence, cells were treated with trypsin–EDTA solution (Sigma, St Louis, MO, USA) and split 1/10 to allow for continuous growth.

Short-term cell viability assays

Hepatocytes were treated for 16 or 32 h with a final concentration of 10 ppb or 10 ppm of 10, 30 or 60 nm size gold nanoparticles. Experiments were carried out to assess cell viability using lactate dehydrogenase assay according to manufacturer's protocol (Cytotoxicity Detection Kit, Mannheim, Germany). Results were compared to negative control cells which received no treatment with nanoparticles.

ROS production

HepG2 cells were seeded in a 6-well plate and incubated overnight in order to allow them to grow. The cells were incubated with 10, 30 or 60 nm size gold nanoparticles at 10 ppb or 10 ppm for 16 or 32 h. ROS overproduction was assessed by including a non-fluorescent probe (H_2DCFDA). This

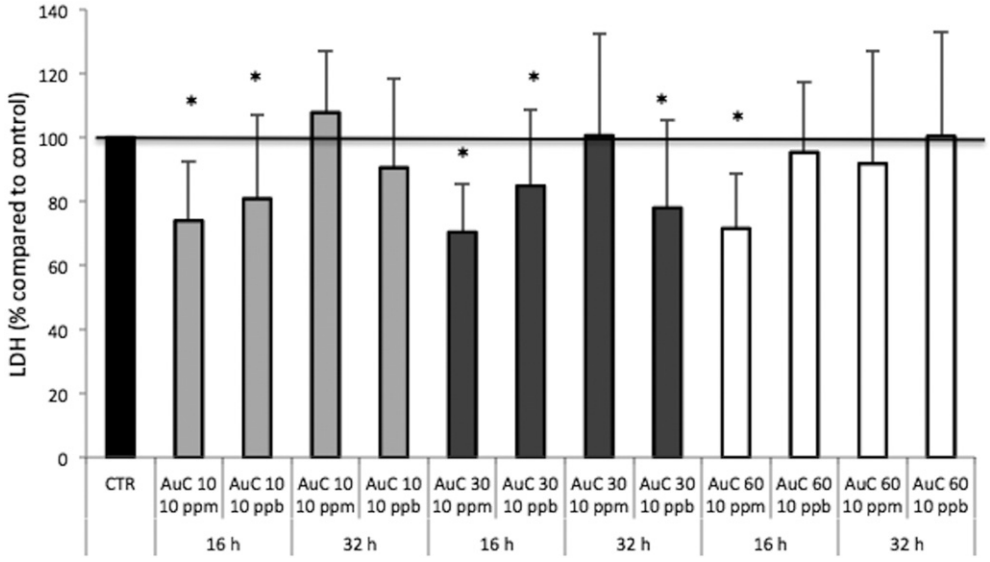

Figure 1. Cell viability assay in hepatic cells. Values shown are means ± SD, CTR (Control cells); AuC 10 (cells treated with 10 nm AuNPs); AuC 30 (cells treated with 30 nm AuNPs); AuC 60 (cells treated with 60 nm AuNPs). *Different from control group. $P < 0.05$.

cell-permeant compound is a chemically reduced form of fluorescein used as an indicator for reactive species in cells. Upon cleavage of the acetate groups by intracellular esterases and oxidation by ROS, the non-fluorescent probe is converted to the highly fluorescent 2′,7′-dichlorofluorescein (DCF). Fluorescence was measured using a microplate reader (Infinitive 200, Tecan, Zürich, Switzerland). The excitation wavelength was set to the absorption maximum (485 nm) and emission was recorded to 538 nm. These results were normalized to cell viability.

Comet assay

HepG2 cells were allowed to grow until 60% confluence was reached. Afterwards, cell cultures were exposed to 10 ppm 10, 30 or 60 nm size gold nanoparticles for 16 h. Positive control cells were treated with 100 mM H_2O_2 for 1 h. Upon treatment, cells were treated with trypsin–EDTA solution (Sigma, St Louis, MO, USA) and centrifuged until getting a pellet. Cells were suspended in 1 mL PBS.

Three microscope glass slides per sample were pre-coated with 1% NMP agarose on one side. 30 μL cell suspension was mixed with 65 μL of LMP agarose solution (final LMP agarose concentration 0.5%). Drops of each agarose-cell suspension were added on each pre-coated slide and placed for 1 h at 4 °C in the lysis solution (containing NaCl 2.225 M, Na_2EDTA 88.9 mM, Tris 8.8 mM, NaOH 0.22 M, 10% DMSO and 1% Triton X-100). Electrophoresis (1 V/cm) was carried out for 20 min at 4 °C using electrophoresis solution (Na_2EDTA 1 mM and NaOH 300 mM, pH > 13). Slides were neutralized three times (5 min every time) with Tris 0.4 M. Ethanol was used to fix slides. Finally, samples were stained with DAPI (1 μg/mL) and analyzed using a fluorescence microscope (Eclipse N*i*; Nikon Instruments Europe B.V., Badhoevedorp, The Netherlands). Over 150 nucleoids per sample (50 nucleoids per slide) stained with DAPI were scored by computerized image analysis, (Comet Assay IV, Perceptive Instrument, Suffolk, UK). DNA damage was determined by comparing moment tails among groups.

Image studies

HT-29 cells were treated with 10 ppm AuNPs for 2, 4 or 16 h in order to determine their subcellular location throughout time. Once the exposure time had finished, cells were prepared to be visualized by TEM.

In vivo studies

Animals

In this experiment, male Wistar rats weighing 190-220 g (Charles River Laboratories, L'Arbresle, France) were randomly divided into four groups. Control group: Eight rats were injected 0.4 mL ultrapure water/day. AuC 10 group: Eight rats were injected 0.4 mL/day 10 nm size gold nanoparticles solution. AuC 30 group: Eight rats were injected 0.4 mL/day 30 nm size gold nanoparticles solution. AuC 60 group: Eight rats were injected 0.4 mL/day 60 nm size gold nanoparticles solution. In all cases, the administration route was intraperitoneal.

All rats were allowed free access to drinking water and diet (the semi-synthetic diet AIN93M)[25] throughout the experimental period. From day 0 of the experiment, all animals were housed in individual metabolic cages designed for the separate collection of feces and urine. The cages were located in a well-ventilated, temperature-controlled room 21 ± 2 °C with relative humidity ranging from 40% to 60%, and a light:dark period of 12 h. On day 9, the rats were anesthetized with a solution of ketamine (0.75 mg kg^{-1} body weight, Fatro Ibérica, Barcelona, Spain) and xylazine (0.10 mg kg^{-1} body weight, Fatro Ibérica, Barcelona, Spain), and exsanguinated by cannulating the posterior aorta. Blood was collected and centrifuged (Beckman, Fullerton, CA, USA) at 3000 rpm for 15 min to separate the serum. The liver,

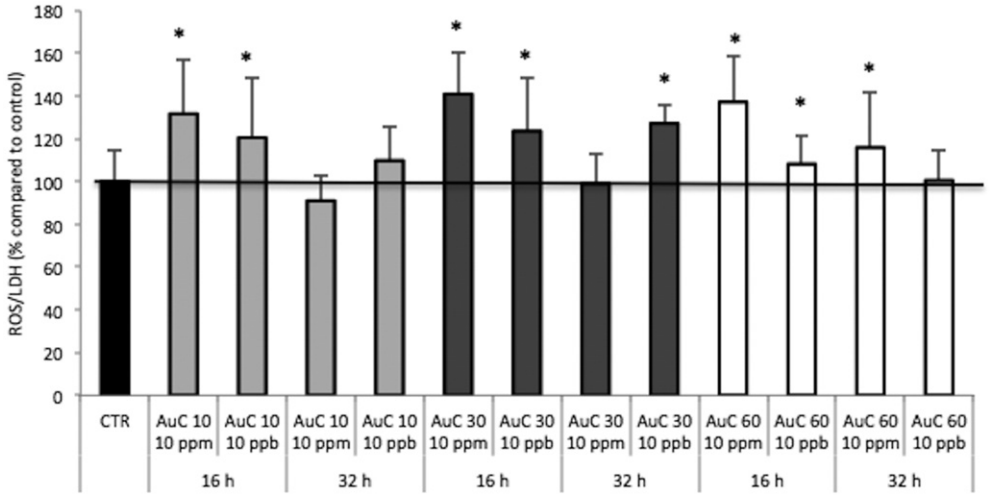

Figure 2. ROS production in hepatic cells. Values shown are means ± SD, CTR (Control cells); AuC 10 (cells treated with 10 nm AuNPs); AuC 30 (cells treated with 30 nm AuNPs); AuC 60 (cells treated with 60 nm AuNPs). *Different from control group. $P < 0.05$.

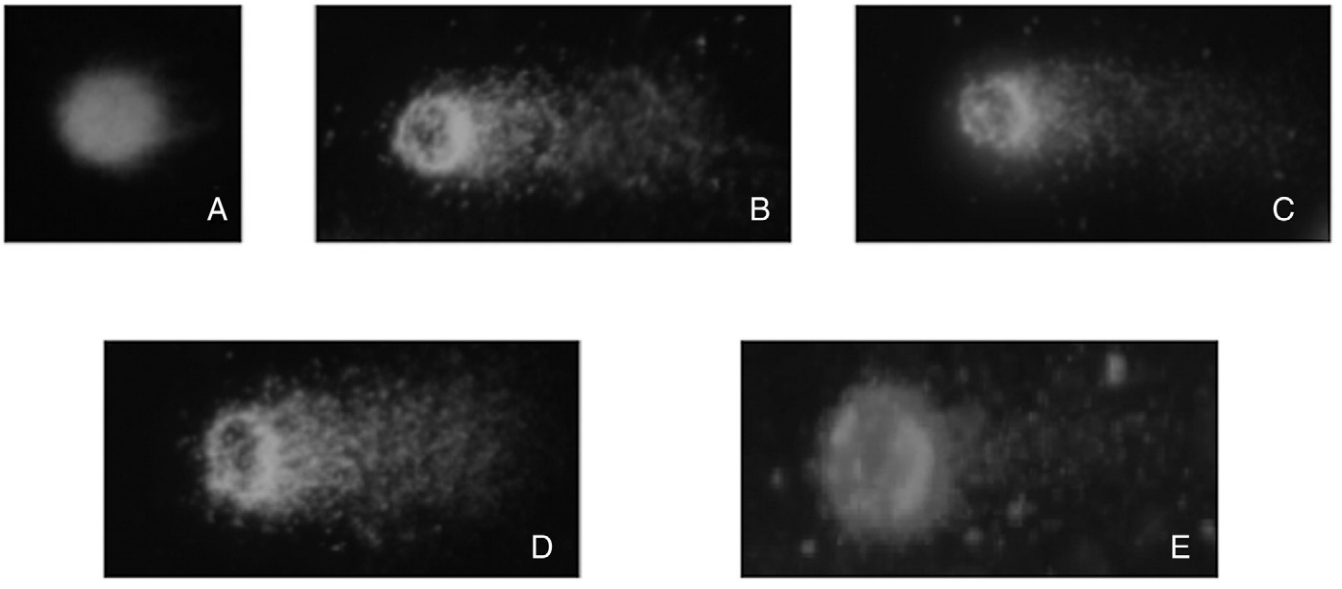

Figure 3. Comets from hepatic cells. (**A**) Cell without treatment; (**B**) cell treated with H_2O_2; (**C**) cell treated with 10 nm AuNPs; (**D**) cell treated with 30 nm AuNPs; (**E**) cell treated with 60 nm AuNPs.

kidney, spleen and intestine were removed, weighed, placed in preweighed polyethylene vials, and stored at −80 °C.

All experiments were undertaken according to Directional Guides Related to Animal Housing and Care (European Community Council, 2010), and the Animal Experimentation Ethics Committee of the University of Granada approved all procedures.

TEM

Intestine cell cultures and liver samples were fixed with fresh primary fixative (1.5% glutaraldehyde, 1.0% formaldehyde in 0.05 M sodium cacodylate buffer, pH 7.4) and post-fixed with secondary fixative (1% osmium tetroxide, 1% potassium ferrocyanide in Milli Q water) followed by dehydration with ascending series of alcohol before embedding samples in epoxy resin. Ultra thin sections were cut and doubly stained with uranyl acetate and lead citrate. A transmission electron microscope LIBRA 120 PLUS microscope at 120 kV (Carl Zeiss SMT., Oberkochen, Germany) was used to determine the fate and uptake of AuNPs into cells.

Liver homogenization

Liver was homogenized in 0.05 M phosphate buffer (pH 7.8) containing 1 g L^{-1} Triton X-100 and 1.34 mM of EDTA using a Micra D-1 homogenizer (ART moderne Labortechnik; Müllheim-Hügelheim, Germany) at 18,000 rpm during 30 s followed by

Table 1
DNA damage in hepatocytes exposed to AuNPs.

	Positive control	AuC 10	AuC 30	AuC 60	Negative control
Moment tail	12.91 ± 6.46	17.45 ± 7.51	8.06 ± 2.88*,†	4.26 ± 6.34*,†	1.38 ± 1.05*,†,‡

Values shown are means ± SD. Positive control (cells treated with H_2O_2); AuC 10 (cells treated with 10 nm AuNPs); AuC 30 (cells treated with 30 nm AuNPs); AuC 60 (cells treated with 60 nm AuNPs); Negative control (cells without treatment).
* Different from positive control group.
† Different from AuC 10.
‡ Different from AuC 30. $P < 0.05$.

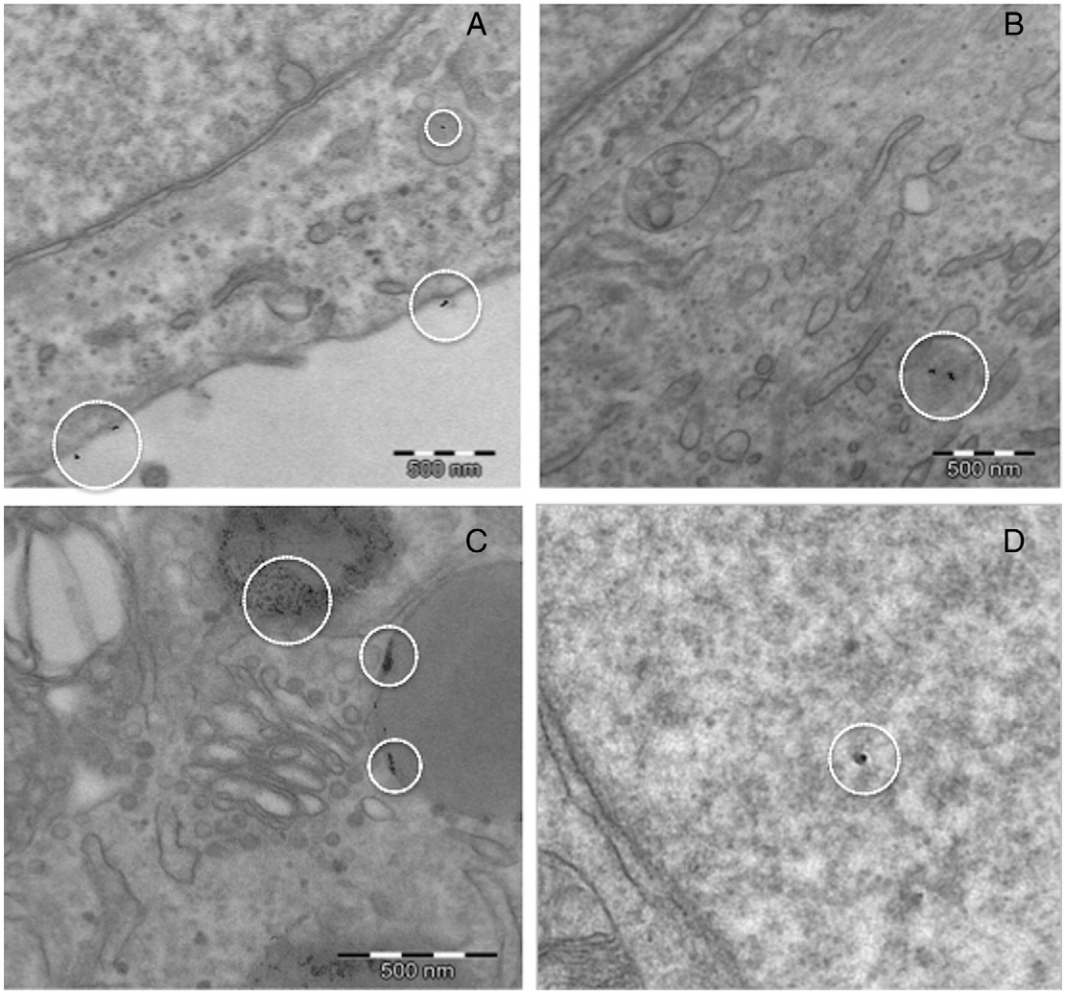

Figure 4. TEM images from colon cells treated with 10 nm AuNPs. (**A**) Nanoparticles are found outside the cell after two hours of administration; (**B**) free AuNPs throughout cytosol after four hours of treatment; (**C**) metabolized nanoparticles are stored in lipid drops after 16 h of treatment; (**D**) AuNP inside the nucleus of a cell.

treatment with Sonoplus HD 2070 ultrasonic homogenizer (Bandelin, Berlin, Germany) at 50% power for 10 s.

Determination of proinflammatory parameters

Interleukin-1β (IL-1β), interleukin-6 (IL-6), interleukin-10 (IL-10) and tumor necrosis factor alpha (TNF-α) levels were determined in liver using the kit Milliplex MAP Rat Cytokine/ Chemokine Magnetic Bead Panel, RECYTMAG-65K, with the Luminex xMAP detection system (EMD, Millipore Corporation, Billerica, MA, USA). The analysis was performed using a Luminex system (Millipore, Germany). Assays were performed according to the manufacturer's instructions.

Determination of biochemical parameters

Glucose, urea, uric acid, triglycerides, albumin, cholesterol, gamma glutamyl transpeptidase (γ-GT), alkaline phosphatase,

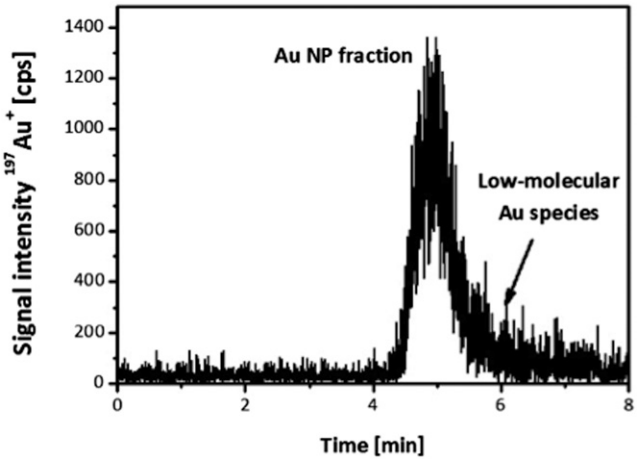

Figure 5. HPLC-ICP-MS chromatogram of a cell extract (HT-29) treated with 10 nm AuNPs.

glutamic oxaloacetic transaminase (GOT) and glutamic pyruvic transaminase (GPT) in plasma were measured with enzymatic colorimetric tests in a Hitachi Modular P autoanalyzer (Roche Diagnostics, Grenzach, Germany).

Determination of protein carbonylation and lipid peroxidation in liver

The levels of protein carbonyl groups were assessed using the Protein Carbonyl Kit (Cayman Chemical Company, MI, USA).

Thiobarbituric acid reactive substances (TBARS), as a marker of lipid peroxidation, were measured by an adaptation of the method of Ohkawa et al in rat liver homogenates.[26]

Gold content in tissues

The extracted organs were previously freeze dried (Cryodos56, Barcelona, Spain). Total gold levels in samples were determined by collision cell ICP-MS (He mode) (Agilent 7700, Waldbronn, Germany) after digestion of the corresponding material using a microwave oven (Milestone, Sorisole, Italy). All the plastic containers used in the analysis were previously cleaned with super-pure nitric acid and ultra-pure water (18.2 Ω) obtained using a Milli Q system (Millipore, Bedford, MA, USA). Samples of dry tissue and fluids were prepared by digestion with aqua regia, using a method from the literature.[12,27–29] When the sample had been digested, the extract was collected and made up to a final volume of 15 mL for subsequent analysis. Calibration curves were prepared following the Rh addition technique as an internal standard, using stock solutions of 1000 mg/L (Merck). The method was validated by recovery studies in samples of organs enriched with Au standards. The percentage of CV obtained was 2.9% for Au. The mean of five separate determinations was used.

Gold speciation in cells and tissues

In addition to total Au determinations, potential degradation of incorporated AuNPs was analyzed. For this, HPLC was coupled online to ICP-MS in order to distinguish between particle-bound Au and Au present as low-molecular complexes. Details on the experimental procedure and the extraction conditions can be found elsewhere[30]

Table 2
Liver damage in rats treated with AuNPs, measured by lipid peroxidation and protein carbonylation (nmol/mg dry tissue).

	Control	AuC 10	AuC 30	AuC 60
TBARS	4.25 ± 0.16	5.73 ± 0.48*	4.83 ± 0.09*	5.22 ± 0.29*
PCG	0.25 ± 0.04	0.67 ± 0.05*	0.53 ± 0.09*	0.69 ± 0.20*

Values shown are means ± SD. TBARS (thiobarbituric acid reactive substances); PCG (protein carbonyl groups); Control (Control rats); AuC 10 (rats treated with 10 nm AuNPs); AuC 30 (rats treated with 30 nm AuNPs); AuC 60 (rats treated with 60 nm AuNPs).
* Different from control group. $P < 0.05$.

Ex vivo stability study

The three sized gold nanoparticles (10, 30 and 60 nm) were incubated at 37 °C in plasma overnight and subsequently observed by TEM in an attempt to assess their stability under physiological solutions *ex vivo*.

Statistical analysis

All variables and indexes were analyzed with descriptive statistics, and the results are reported as the mean and standard deviation. Statistical comparisons among the groups were performed by the Mann–Whitney test, a nonparametric testing for unrelated samples. For the bivariate analysis, Spearman's coefficient of correlation was calculated. All analyses were carried out with the version 20.0 of the Statistical Package for Social Sciences (SPSS Inc., Chicago, IL). Differences were considered significant at the 5% probability level.

Results

In vitro

Cell viability assay

Figure 1 shows lactate dehydrogenase assay in HepG2 cells. The AuNPs provoked a decrease in viability at 16 h, compared to the control group. This viability tended to normalize after 32 h. No significant differences were found regarding the size of the nanoparticles.

ROS production

The effect of AuNPs on the generation of ROS was confirmed after observing an increase in every sample treated with 10 ppm AuNPs at 16 h, as shown in Figure 2. This overproduction was normalized after 32 h of treatment. As expected, these results agree with those related to cell viability; thus revealing a growth in cell mortality as the ROS production increases.

AuNPs-induced oxidative damage to DNA

Images from the comet assay in hepatocytes are presented in Figure 3. Moment tail measurements showed that there was a significant increase in the DNA damage of all treated groups compared to the negative control cells, as shown in Table 1. In fact, the smaller the nanoparticle size, the higher the damage observed. No significant differences were found between the positive control cells and the cell culture treated with 10 nm AuNPs. 30 and 60 nm AuNPs caused higher increases of moment tail compared to the negative control cells, although these increases were lower than the positive control group.

Table 3
Gold content in different tissues and fluids (μg/kg tissue).

	Control	AuC 10	AuC 30	AuC 60
Liver	0.57 ± 0.17	785.64 ± 385.64*	1289.32 ± 694.72*	325.61 ± 164.95*,†,‡
Kidney	0.59 ± 0.19	595.89 ± 392.02*	603.92 ± 554.77*	67.81 ± 39.21*,†,‡
Intestine	0.87 ± 0.32	1301.55 ± 320.30*	648.21 ± 301.61*	413.56 ± 307.37*,†
Spleen	0.96 ± 0.47	945.39 ± 514.33*	2602.41 ± 731.85*	7938.57 ± 455.71*,†,‡
Feces	0.34 ± 0.12	75.81 ± 62.38*	77.94 ± 59.40*	33.86 ± 30.80*
Urine	0.18 ± 0.11	3.55 ± 1.71*	4.18 ± 1.43*	2.22 ± 1.34*

Values shown are means ± SD. Control (Control rats); AuC 10 (rats treated with 10 nm AuNPs); AuC 30 (rats treated with 30 nm AuNPs); AuC 60 (rats treated with 60 nm AuNPs).
* Different from control group;
† Different from AuC 10;
‡ Different from AuC 30. $P < 0.05$.

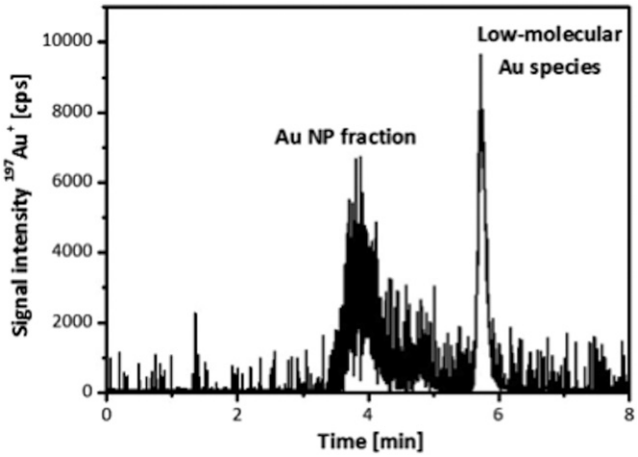

Figure 6. HPLC-ICP-MS chromatogram of an extract of rat tissue after injection of 30 nm AuNPs.

Image studies

Three different exposure periods were tested in colon cells in order to determine the effect of time on subcellular location and possible degradation of AuNPs. Images shown in Figure 4 revealed that in early stages after the exposure to the nanoparticles, they are easily found throughout cytosol and extracellular spaces. However, AuNPs were relocated along time, being found in nucleus and lipid drops after 16 h of exposure.

Gold speciation

A potential degradation of AuNPs was monitored by HPLC-ICP-MS. Figure 5 represents a typical chromatogram obtained from a cell extract (HT-29) after incubation with 10 nm AuNPs for 16 h. Besides the expected nanoparticle fraction, no low-molecular Au species could be detected.

In vivo

Evaluation of the lipid peroxidation

TBARS measurements indicate that the treatment with AuNPs caused a significant rise in lipid peroxidation. As observed in Table 2, the increase was slightly higher in those rats treated with 10 nm AuNPs.

Influence of AuNPs on protein carbonylation

The administration of AuNPs caused a significant rise in the protein carbonyl groups formation, compared to the control groups (see Table 2). No differences were found among the treated groups.

Gold content in rat organs

Table 3 shows the total gold content in liver, kidney, intestine, spleen, feces and urine.

ICP-MS measurements in the liver and kidney showed that the rats treated with 10 and 30 nm AuNPs accumulated the highest concentration of gold, showing no significant differences between both groups. Lower content of gold was found in the group treated with 60 nm AuNPs, although it is significantly higher than the control animals.

In relation to the intestine, a very marked, significant increase was observed in the gold levels after injecting the three studied nanoparticles, even though the administration route was not enteral but intraperitoneal. Especially relevant was the very strong presence of 10 nm AuNPs in this tissue.

In accordance with the other organs, all exposed rats showed significantly higher content of gold in the spleen. Especially remarkable was the amount of gold in the rats treated with the 60 nm size AuNPs. In contrast with the rest of analyzed organs, the spleen was the unique organ where the deposits of gold in those animals treated with 60 nm AuNPs were higher.

In relation to the excreta, although significant levels of gold were detected in 24 h urine of exposed rats compared to the untreated group, urine resulted not to be the main excretion route in any of the studied AuNPs sizes, as the results showed that the concentration of gold in feces was much higher, especially when the administrated AuNPs sizes were 10 and 30 nm.

HPLC-ICP-MS analyses revealed the presence of low-molecular Au species.[30] Figure 6 shows a chromatogram of an extract from rat tissue after treatment with 30 nm AuNPs.

TEM images

After administering the nanoparticles to the animals, slides of liver samples were observed by transmission electron microscopy. As shown in Figure 7, AuNPs were stored in lipid drops; although the size of these nanoparticles was smaller than the original ones (~6-8 nm). Some single, non-aggregated AuNPs were also found dispersed throughout the cytosol.

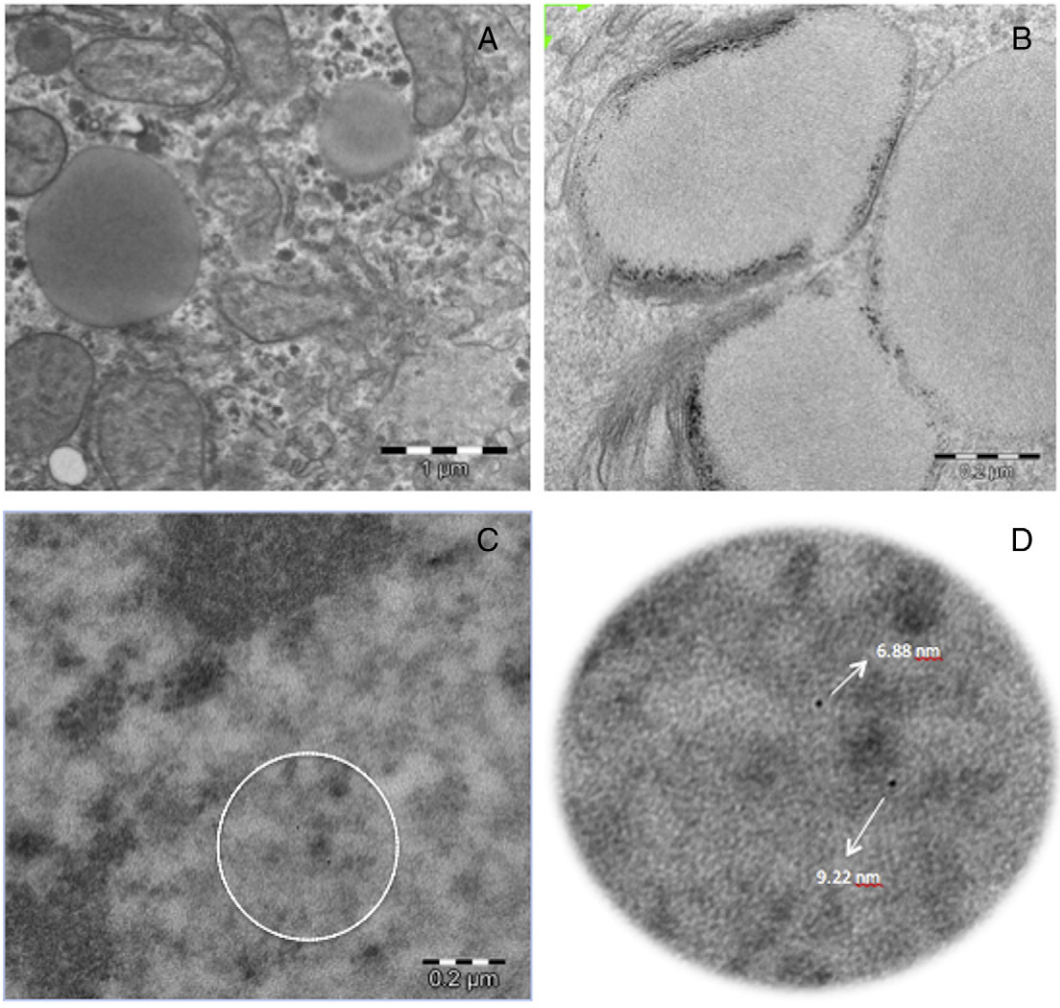

Figure 7. TEM images from hepatocytes of untreated rats (**A**) *versus* rats treated with AuC 10 (**B**, **C** and **D**). (**A**) Subcellular structures with clean lipid drops among them; (**B**) lipid drops with small nanoparticle); (**C**) nucleus from a cell with two nanoparticles inside it; (**D**) enlargement from image **C**, with the sizes of two nanoparticles.

Table 4
Inflammatory parameters in liver (pg/mg tissue).

	Control	AuC 10	AuC 30	AuC 60
TNF-α	0.088 ± 0.012	0.091 ± 0.010	0.097 ± 0.096	0.096 ± 0.012
IL-1β	0.88 ± 0.15	0.77 ± 0.03	0.80 ± 0.07	0.82 ± 0.05
IL-6	11.82 ± 2.57	11.84 ± 2.47	11.54 ± 1.31	11.40 ± 1.06
IL-10	1.48 ± 0.22	1.31 ± 0.08	1.35 ± 0.10	1.34 ± 0.17

Values shown are means ± SD. Control (Control rats); AuC 10 (rats treated with 10 nm AuNPs); AuC 30 (rats treated with 30 nm AuNPs); AuC 60 (rats treated with 60 nm AuNPs).

In the case of the organs exposed to 10 nm AuNPs, some nanoparticles were able to cross the nucleus membrane and were found inside it.

Inflammatory parameters

Table 4 represents the values of four different inflammatory markers that were measured in liver: TNF-α, IL-1β, IL-6 and IL-10. No significant changes were found in any case regarding these factors.

Biochemical parameters

Several biochemical factors that were measured in this experiment are shown in Table 5: glucose, urea, uric acid, triglycerides, albumin, cholesterol, γ-GT, alkaline phosphatase, GOT and GPT. Data support that no changes took place in rats treated with AuNPs compared to control group.

Ex vivo stability study

After incubating the gold nanoparticles in plasma, a tendency to aggregation was observed, but did not affect to the diameters of the nanoparticles, as observed in Figure 8. Nevertheless, regardless the aggregation state in external solutions, this tendency was not observed in those nanoparticles present in tissues of the treated rats, and it did not have a final effect on the uptake of the nanoparticles into cells, as shown by the *in vitro* and *in vivo* TEM images.

Correlations

The bivariate study revealed the existence of a significant relationship, among which the following are particularly

Table 5
Biochemical markers measured in plasma.

	Control	AuC 10	AuC 30	AuC 60
Glucose (mg/dL)	143.75 ± 17.99	207.25 ± 88.80	147.75 ± 16.68	137 ± 22.01
Urea (mg/dL)	30.75 ± 3.30	18.75 ± 6.40	24.50 ± 2.38	27.00 ± 1.41
Uric acid (mg/dL)	0.9 ± 0.2	0.8 ± 0.1	1.0 ± 0.3	0.9 ± 0.3
Triglycerides (mg/dL)	98.5 ± 20.02	113.25 ± 43.96	111.00 ± 16.45	94.75 ± 24.93
Cholesterol (mg/dL)	46.75 ± 2.99	56.75 ± 14.57	60.25 ± 5.56	55.00 ± 8.79
Albumin (g/L)	30.25 ± 1.71	30.25 ± 1.26	28.25 ± 0.96	29.25 ± 2.06
γ-GT (U/L)	<3	<3	<3	<3
Alkaline phosphatase (U/L)	175.00 ± 54.84	205.75 ± 49.22	169.00 ± 50.21	175.00 ± 51.31
GOT (U/L)	82.25 ± 4.42	77.50 ± 7.42	80.25 ± 5.85	84.25 ± 9.60
GPT (U/L)	17.75 ± 1.71	18.00 ± 3.56	18.00 ± 2.45	17.00 ± 3.65

Values shown are means ± SD. γ-GT (gamma glutamyl transpeptidase); GOT (glutamic oxaloacetic transaminase); GPT (glutamic pyruvic transaminase); Control (Control rats); AuC 10 (rats treated with 10 nm AuNPs); AuC 30 (rats treated with 30 nm AuNPs); AuC 60 (rats treated with 60 nm AuNPs).

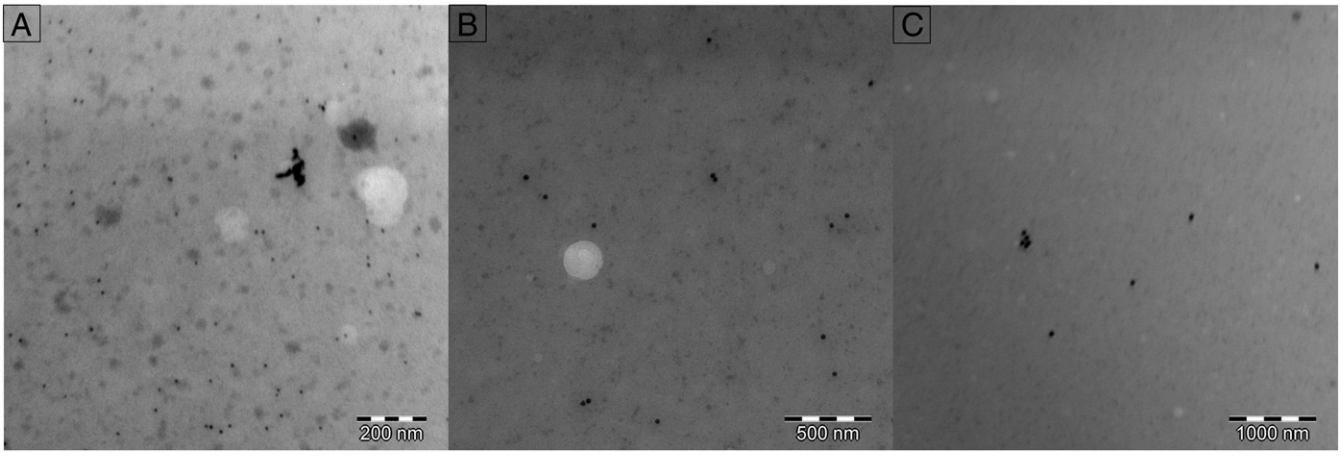

Figure 8. *Ex vivo* stability studies of (**A**) 10 nm diameter, (**B**) 30 nm diameter and (**C**) 60 nm diameter nanoparticles. TEM study shows the tendency of AuNP to aggregation.

important: AuNPs size correlated positively with gold content in spleen ($r = 0.895$; $P < 0.01$); AuNPs size correlated negatively with gold content in kidney ($r = -0.837$; $P < 0.01$); AuNPs size correlated negatively with gold content in intestine ($r = -0.736$; $P < 0.05$).

Discussion

Gold nanoparticles have been found to be useful in a wide range of applications, like the delivery and controlled release of a variety of chemical agents including anticancer drugs, antibiotics, amino acids, peptides, glucose, antioxidants, nucleic acids, and isotopes.[13] However, the increase in their use has raised concerns about the possible interactions *in vivo* and the unexpected responses inside humans and other living organisms.[31] Thus, the aim of this study was to determine the tissue distribution, subcellular location and deleterious effects of three different sizes of AuNPs both *in vitro* and *in vivo*. The results obtained from this study confirm that these nanoparticles are accumulated in the organs and provoke an incipient oxidative damage, although various mechanisms seem activated to neutralize the deleterious effects that occur after administration of the particles.

Gold nanoparticles have been related to imbalances in oxidative status *in vitro*.[32,33] In the present study, hepatocytes (HepG2 cells) were used due to the key role of the liver in metabolic processes and detoxification in the organism. The results show that the exposure of hepatocytes to AuNPs caused a time and dose-dependent increase in ROS production. This increase seems to be time and dose-dependent. Only slight impairments on the oxidative status were found 32 h after the exposure, whereas 16 h caused a growth in ROS production in both 10 ppb and 10 ppm. Although there are no significant differences, the highest dose of AuNPs tended to provoke more damage. These results support those obtained from the cell viability assay that showed a rise in cell mortality. Thereby, it is clear that AuNPs are able to induce an initial oxidative damage, but cells manage to control the ROS overproduction after 32 h of exposure, probably by means of the increase in the antioxidant activity.[15]

After confirming that gold nanoparticles were able to cause oxidative damage measured by ROS production at 16 h and 10 ppm, comet assay was used in order to assess whether this ROS

overproduction caused DNA damage[34,35] under the same conditions. Tail moment measurements proved that AuNPs induced DNA breaks. Furthermore, the produced damage increased as the nanoparticle size decreased.[36] Thus, cell culture exposed to 60 nm gold nanoparticles showed no differences compared to the negative control cells, whereas HepG2 cells treated with 10 nm AuNPs showed moment tails similar to those from the positive control, where cells were exposed to hydrogen peroxide. Taking into account that the effective diameter of the nucleus pore is around 35 nm,[37] it is probable that the 10 and 30 nm nanoparticles were able to cross the nucleus membrane, thus favoring the DNA breaks. This fact was confirmed by TEM images obtained in the liver of the rats, where several nanoparticles were found inside the nucleus after treatment with 10 nm AuNPs.

Lipid peroxidation and protein carbonylation have been widely measured in experiments with AuNPs in order to determine the damage in lipids and proteins caused by oxidative stress.[8,10,14,38] In our case, the levels of malondialdehyde and protein carbonyl groups were found to be increased in livers of the exposed rats compared to the control group. These results indicate the increased production of free radicals in this organ, which became concomitant with the increased production of TBARS and protein carbonyl groups.

In previous studies performed by other authors, AuNPs were observed by TEM, showing different patterns depending on the properties of the nanoparticles and the experimental conditions.[17,39–41] In our study, although gold nanoparticles tended to aggregate when incubated with plasma *ex vivo*, this tendency was not detected *in vitro* or *in vivo*. Single nanoparticles were found inside the cells in all cases. Similar results have been widely described elsewhere.[39,41] In our view, the complexity of the biological systems may justify the differences found *ex vivo* and *in vitro*. Several reasons may have determined this fact: the multiple membranes that gold nanoparticles must individually cross (endothelium and vascular membrane, cell membrane, *etc.*); or even the agitation process derived from myocardium activity may be involved.

The fact that some intact nanoparticles were detected throughout the cytosol and that they were found in a smaller size than the originally administered also included inside lipid drops, led us to consider that the nanoparticles are somehow digested or metabolized by biological or chemical mechanisms before being neutralized and stored in the lipid drops in an attempt to reduce the toxicity in the liver. This hypothesis was confirmed by the detection of low-molecular Au species in the organs (Figure 6). In our opinion, this degradation process could be based on the phagocytic activity of macrophages mainly from spleen (where high levels of gold were found in our study), or liver Kupffer cells, as described by other authors.[42,43] Thus, the enzymatic compounds from the lysosomes of the macrophages would act by digesting the gold nanoparticles.

We tried to confirm these results in other type of cells involved in the biodistribution of the AuNPs, the colon cells HT-29. For that purpose, and in another to try to observe the uptake mechanism of the AuNPs into the cell, we exposed this cell line to AuNPs in the same conditions as the HepG2 line, but at different exposure times. In this experiment, images revealed that in the early stages nanoparticles are easily found throughout cytosol and extracellular spaces. However, along time AuNPs were relocated, being found in lipid drops and inside the nucleus after 16 h of exposure. No degradation was observed (Figure 5).

Results show that there is an unequal distribution of Au depending on the size of the administered nanoparticle. The quantitative ICP-MS measurements indicate that gold is accumulated in all the studied tissues of every treated group.[12,28,44] In fact, liver, kidney and intestine show the same pattern, where 10 and 30 nm AuNPs seem to accumulate more in those three organs than 60 nm AuNPs; whereas 60 nm AuNPs mostly accumulate in spleen (Table 3). Thus, 10 nm AuNPs were mainly accumulated in intestine, followed by spleen, liver and kidney to a lesser extent. Meanwhile, 30 nm AuNPs tended to accumulate in spleen, followed by liver, intestine and kidney. Finally, when gold was administered as 60 nm AuNPs, the highest accumulation was observed in the spleen, followed by the intestine, liver and kidney. It has been previously suggested that when AuNPs size is larger than renal filtration cutoff,[45] nanoparticles are not excreted in urine; instead they are eliminated from the blood by the reticuloendothelial system and thus tend to accumulate in the spleen and liver.[14] Therefore, the spleen would be a key organ in the AuNPs metabolism. Our results also showed that the bigger the size of the administered nanoparticle was, the more accumulation was found in the spleen. The opposite effect was observed in the intestine, where the accumulation was higher as the size of the AuNPs decreased. The results obtained for the bivariate correlations support these results (see results). In this sense, the high levels of gold in intestine, together with the increase in gold concentration measured in feces, and taking into account that the administration route of the nanoparticles was intraperitoneal (and not enteral), prove that fecal is the main endogenous route of elimination of the nanoparticles. Moreover, the results obtained in 24 h urine showed much lower Au levels among treated rats, excluding the urine as a main *via* of excretion for AuNPs.

As exposed in the results section, the treatment with AuNPs did not modify the levels of inflammatory or biochemical tissue damage markers in plasma, compared to the control group. The absence of any effect after several days of treatment has been formerly observed by other authors.[46–49] In our view, although AuNPs caused an increase in ROS production and as a result it increased the damage in proteins and lipids, it was insufficient to trigger an inflammatory response and therefore tissue damage.

The obtained results led us to conclude that the size of the nanoparticles determines differences in their metabolic fate and in the formation of deposits in the different biological systems. The size of the nanoparticles also determines their excretion route, being the main *via* of the nanoparticles with the highest diameter the reticuloendothelial system of the spleen, and the intestinal endogenous *via* the main route of excretion of the nanoparticles with the smallest size. Furthermore, we have proved that gold nanoparticles provoke an imbalance in the oxidative status of the cells, which is accompanied by damage in the genetic, lipid and protein structures. These alterations presented a clear size-dependence, as the 10 nm AuNPs showed more injurious effects, detected by their nuclear location and their higher DNA damage. In spite of these oxidative induced

deleterious structural effects, it was not found alterations on the inflammatory status nor tissue damage after this short period of exposure to AuNPs. These results allow us to consider the gold nanoparticles as feasible tools for the short-term clinic use. Nevertheless, in light of the evidence regarding their harmful effects in the genetic material, together with the formation of the deposits of gold in several organs, we strongly recommend to address a deeper study about the use of AuNPs as drug delivery vehicle in the chronic treatment of diseases as cancer or diabetes. Furthermore, the convenience of the chronic exposure of the particles in fields like cosmetics, textile or electronics must be assessed, with special mention to those particles with the smallest size, which presented the most deleterious effects.

References

1. Han YD, Park YM, Chun HJ, Yoon HC. A low-cost optical transducer utilizing common electronics components for the gold nanoparticle-based immunosensing application. *Chem* 2015;**220**:233-42.
2. Chen L, Wang S, Han C, Cheng Y, Qian L. Performance improvement of inverted polymer solar cells by incorporating au and ZnO nanoparticles bilayer plasmonic nanostructure. *Synth Met* 2015;**209**:544-8.
3. Nita R, Trammell SA, Ellis GA, Moore MH, Soto CM, Leary DH, et al. Kinetic analysis of the hydrolysis of methyl parathion using citrate-stabilized 10 nm gold nanoparticles. *Chemosphere* 2016;**144**:1916-9.
4. Ngwa W, Kumar R, Sridhar S, Korideck H, Zygmanski P, Cormack RA, et al. Targeted radiotherapy with gold nanoparticles: current status and future perspectives. *Nanomedicine* 2014;**9**:1063-82.
5. Feliu N, Docter D, Heine M, del Pino P, Ashraf S, Kolosnjaj-Tabi J, et al. In vivo degeneration and the fate of inorganic nanoparticles. *Chem Soc Rev* 2016;**45**:2440-57.
6. Muddineti OS, Ghosh B, Biswas S. Current trends in using polymer coated gold nanoparticles for cancer therapy. *Pharm* 2015;**484**:252-67.
7. Yamada M, Foote M, Prow TW. Therapeutic gold, silver, and platinum nanoparticles. *Wiley Interdiscip Rev Nanomed Nanobiotechnol* 2015;**7**:428-45.
8. Thakor AS, Paulmurugan R, Kempen P, Zavaleta C, Sinclair R, Massoud TF, et al. Oxidative stress mediates the effects of Raman-active gold nanoparticles in human cells. *Small* 2011;**7**:126-36.
9. Connor EE, Mwamuka J, Gole A, Murphy CJ, Wyatt MD. Gold nanoparticles are taken up by human cells but do not cause acute cytotoxicity. *Small* 2005;**1**:325-7.
10. Abdelhalim MAA-K, Al-Ayed MS, Moussa SA. The effects of intraperitoneal administration of gold nanoparticles size and exposure duration on oxidative and antioxidants levels in various rat organs. *Pharm Sci* 2015;**28**:705-12.
11. Geiser M, Rothen-Rutishauser B, Kapp N, Schürch S, Kreyling W, Schulz H, et al. Ultrafine particles cross cellular membranes by nonphagocytic mechanisms in lungs and in cultured cells. *Environ Health Perspect* 2005;**113**:1555-60.
12. De Jong WH, Hagens WI, Krystek P, Burger MC, Sips AJAM, Geertsma RE. Particle size-dependent organ distribution of gold nanoparticles after intravenous administration. *Biomaterials* 2008;**29**:1912-9.
13. Khan HA, Abdelhalim MAK, Alhomida AS, Al Ayed MS. Short communication transient increase in IL-1β, IL-6 and TNF-α gene expression in rat liver exposed to gold nanoparticles. *Genet Mol Res* 2013;**12**:5851-7.
14. Abdelhalim MAK. Uptake of gold nanoparticles in several rat organs after intraperitoneal administration in vivo: a fluorescence study. *Biomed Res Int* 2013;**2013**:353695.
15. Li JJ, Hartono D, Ong C-N, Bay B-H, Yung L-YL. Autophagy and oxidative stress associated with gold nanoparticles. *Biomaterials* 2010;**31**:5996-6003.
16. Li JJ, Zou L, Hartono D, Ong C-N, Bay B-H, Lanry Yung L-Y. Gold nanoparticles induce oxidative damage in lung fibroblasts in vitro. *Adv Mater* 2008;**20**:138-42.
17. Nelson BC, Petersen EJ, Marquis BJ, Atha DH, Elliott JT, Cleveland D, et al. NIST gold nanoparticle reference materials do not induce oxidative DNA damage. *Nanotoxicology* 2013;**7**:21-9.
18. Negahdary M, Chelongar R, Zadeh SK, Ajdary M. The antioxidant effects of silver, gold, and zinc oxide nanoparticles on male mice in in vivo condition. *Adv Biomed Res* 2015;**4**:69-74.
19. Nativo P, Prior IA, Brust M. Uptake and intracellular fate of surface-modified gold nanoparticles. *ACS Nano* 2008;**2**:1639-44.
20. Yen H-J, Hsu S-H, Tsai C-L. Cytotoxicity and immunological response of gold and silver nanoparticles of different sizes. *Small* 2009;**5**:1553-61.
21. Lai T-H, Shieh J-M, Tsou C-J, Wu W-B. Gold nanoparticles induce heme oxygenase-1 expression through Nrf2 activation and Bach1 export in human vascular endothelial cells. *Nanomedicine* 2015;**10**:5925-39.
22. Khan HA, Ibrahim KE, Khan A, Alrokayan SH, Alhomida AS, Lee Y. Comparative evaluation of immunohistochemistry and real-time PCR for measuring proinflammatory cytokines gene expression in livers of rats treated with gold nanoparticles. *Exp Toxicol Pathol* 2016;**68**:381-90.
23. Abdelhalim MAK, Abdelmottaleb Moussa SA. The gold nanoparticle size and exposure duration effect on the liver and kidney function of rats: in vivo. *Biol Sci* 2013;**20**:177-81.
24. Katsnelson BA, Privalova LI, Gurvich VB, Makeyev OH, Shur VY, Beikin YB, et al. Comparative in vivo assessment of some adverse bioeffects of equidimensional gold and silver nanoparticles and the attenuation of nanosilver's effects with a complex of innocuous bioprotectors. *Mol Sci* 2013;**14**:2449-83.
25. Reeves PG, Nielsen FH, Fahey GC. AIN-93 purified diets for laboratory rodents: final report of the American Institute of Nutrition ad hoc writing committee on the reformulation of the AIN-76A rodent diet. *J Nutr* 1993;**123**:1939-51.
26. Ohkawa H, Ohishi N, Yagi K. Assay for lipid peroxides in animal tissues by thiobarbituric acid reaction. *Anal Biochem* 1979;**95**:351-8.
27. Sonavane G, Tomoda K, Makino K. Biodistribution of colloidal gold nanoparticles after intravenous administration: effect of particle size. *Biointerfaces* 2008;**66**:274-80.
28. Loeschner K, Brabrand MSJ, Sloth JJ, Larsen EH. Use of alkaline or enzymatic sample pretreatment prior to characterization of gold nanoparticles in animal tissue by single-particle ICPMS. *Anal Bioanal Chem* 2013;**406**:3845-51.
29. Wang M, Zheng L-N, Wang B, Chen H-Q, Zhao Y-L, Chai Z-F, et al. Quantitative analysis of gold nanoparticles in single cells by laser ablation inductively coupled plasma-mass spectrometry. *Anal Chem* 2014;**86**:10252-6.
30. Soto-Alvaredo J, López-Chaves C, Sánchez-Gonzalez C, Montes-Bayón M, Llopis J, Bettmer J. Speciation of gold nanoparticles and low molecular gold species in Wistar rat tissues by HPLC coupled to ICP-MS. *J Anal At Spectrom* 2017;**32**:193-9.
31. Fernández-Iglesias N, Bettmer J. Complementary mass spectrometric techniques for the quantification of the protein corona: a case study on gold nanoparticles and human serum proteins. *Nanoscale* 2015;**7**:14324-31.
32. Piryazev AP, Azizova OA, Aseichev AV, Dudnik LB, Sergienko VI. Effect of gold nanoparticles on production of reactive oxygen species by human peripheral blood leukocytes stimulated with opsonized zymosan. *Bull Exp Biol Med* 2013;**156**:101-3.
33. Mateo D, Morales P, Ávalos A, Haza AI. Oxidative stress contributes to gold nanoparticle-induced cytotoxicity in human tumor cells. *Toxicol Mech Methods* 2014;**24**:161-72.
34. Paino IMM, Marangoni VS, de Oliveira R de CS, Antunes LMG, Zucolotto V. Cyto and genotoxicity of gold nanoparticles in human

hepatocellular carcinoma and peripheral blood mononuclear cells. *Toxicol Lett* 2012;**215**:119-25.
35. Chueh PJ, Liang R-Y, Lee Y-H, Zeng Z-M, Chuang S-M. Differential cytotoxic effects of gold nanoparticles in different mammalian cell lines. *J Hazard Mater* 2014;**264**:303-12.
36. Xia Q, Li H, Liu Y, Xiao K. The effect of particle size on the genotoxicity of gold nanoparticles. *J Biomed Mater Res A* 2016, http://dx.doi.org/10.1002/jbm.a.35944.
37. Wente SR, Rout MP. The nuclear pore complex and nuclear transport. *Cold Spring Harb Perspect Biol* 2010;**2**:a000562.
38. Ferreira GK, Cardoso E, Vuolo FS, Michels M, Zanoni ET, Carvalho-Silva M, et al. Gold nanoparticles alter parameters of oxidative stress and energy metabolism in organs of adult rats. *Biochem Cell Biol* 2015;**93**:548-57.
39. Yang X, Yang M, Pang B, Vara M, Xia Y. Gold nanomaterials at work in biomedicine. *Chem Rev* 2015;**115**:10410-88.
40. Zhang Q, Ma Y, Yang S, Xu B, Fei X. Small-sized gold nanoparticles inhibit the proliferation and invasion of SW579 cells. *Mol Med Rep* 2015;**12**:8313-9.
41. Tlotleng N, Vetten MA, Keter FK, Skepu A, Tshikhudo R, Gulumian M. Cytotoxicity, intracellular localization and exocytosis of citrate capped and PEG functionalized gold nanoparticles in human hepatocyte and kidney cells. *Cell Biol Toxicol* 2016;**32**:305-21.
42. Dragoni S, Franco G, Regoli M, Bracciali M, Morandi V, Sgaragli G, et al. Gold nanoparticles uptake and cytotoxicity assessed on rat liver precision-cut slices. *Toxicol Sci* 2012;**128**:186-97.
43. Sadauskas E, Danscher G, Stoltenberg M, Vogel U, Larsen A, Wallin H. Protracted elimination of gold nanoparticles from mouse liver. *Nanomedicine* 2009;**5**:162-9.
44. Simpson CA, Salleng KJ, Cliffel DE, Feldheim DL. In vivo toxicity, biodistribution, and clearance of glutathione-coated gold nanoparticles. *Nanomedicine* 2013;**9**:257-63.
45. Chen F, Goel S, Hernandez R, Graves SA, Shi S, Nickles RJ, et al. Dynamic positron emission tomography imaging of renal clearable gold nanoparticles. *Small* 2016;**12**:2775-82.
46. Downs TR, Crosby ME, Hu T, Kumar S, Sullivan A, Sarlo K, et al. Silica nanoparticles administered at the maximum tolerated dose induce genotoxic effects through an inflammatory reaction while gold nanoparticles do not. *Mutat Res Toxicol Environ Mutagen* 2012;**745**:38-50.
47. Khan HA, Abdelhalim MAK, Alhomida AS, Al-Ayed MS. Effects of naked gold nanoparticles on proinflammatory cytokines mRNA expression in rat liver and kidney. *Biomed Res Int* 2013;**2013**:590730.
48. Sousa AA, Hassan SA, Knittel LL, Balbo A, Aronova MA, Brown PH, et al. Biointeractions of ultrasmall glutathione-coated gold nanoparticles: effect of small size variations. *Nanoscale* 2016;**8**:6577-88.
49. Yang C, Yang H, Wu J, Meng Z, Xing R, Tian A, et al. No overt structural or functional changes associated with PEG-coated gold nanoparticles accumulation with acute exposure in the mouse heart. *Toxicol Lett* 2013;**222**:197-203.